Electronic Supplementary Material (ESI) for CrystEngComm.

SUPPORTING INFORMATION

Centroid…centroid and hydrogen bond interactions as robust supramolecular units for crystal engineering: X-ray crystallographic, computational and urease inhibitory investigations of 1,2,4-triazolo[3,4-a]phthalazines

Sumera Zaib,[a] Aliya Ibrar,[b] Marriyam Ramay,[a] Shabab Zahra,[a] Tuncer Hökelek,[c] Jim Simpson,[d] Christopher John McAdam,[d] Nasser S. Awwad,[e] Hala A. Ibrahium,[f,g] Antonio Frontera,[h,*] Imtiaz Khan,[i,*]

[a]Department of Biochemistry, Faculty of Life Sciences, University of Central Punjab, Lahore 54590, Pakistan

[b]Department of Chemistry, Faculty of Life Science, The University of Haripur, KPK 22620, Pakistan

[c]Department of Physics, Hacettepe University, Beytepe-Ankara, 06800, Turkey

[d]Department of Chemistry, University of Otago, P.O. Box 56, Dunedin, 9054, New Zealand

[e]Chemistry Department, Faculty of Science, King Khalid University, P.O. Box 9004, Abha 61413, Saudi Arabia

[f]Biology Department, Faculty of Science, King Khalid University, P.O. Box 9004, Abha 61413, Saudi Arabia

[g]Department of Semi Pilot Plant, Nuclear Materials Authority, P.O. Box 530, El Maadi, Egypt

[h]Department de Química, Universitat de les Illes Balears, Crta de Valldemossa km 7.5, 07122 Palma de Mallorca (Baleares), Spain

[i]Department of Chemistry and Manchester Institute of Biotechnology, The University of Manchester, 131 Princess Street, Manchester M1 7DN, United Kingdom

Corresponding authors: toni.frontera@uib.es (A.F.); kimtiaz@hotmail.co.uk (I.K.)

SUPPORTING INFORMATION

Hirshfeld surface analysis

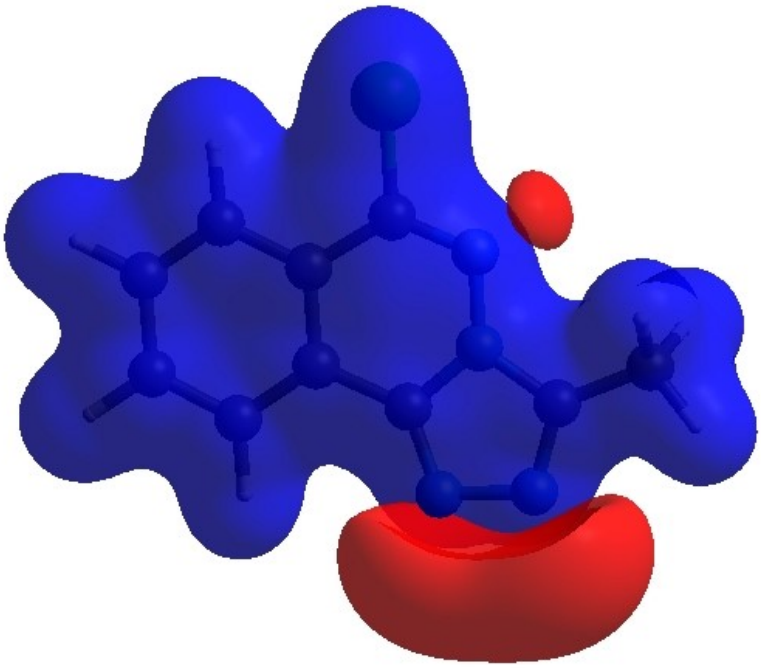

Fig. S1. View of the three-dimensional Hirshfeld surface of compound **5** plotted over electrostatic potential energy in the range -0.0500 to 0.0500 a.u. using the STO-3 G basis set at the Hartree–Fock level of theory. Hydrogen-bond donors and acceptors are shown as blue and red regions around the atoms corresponding to positive and negative potentials, respectively.

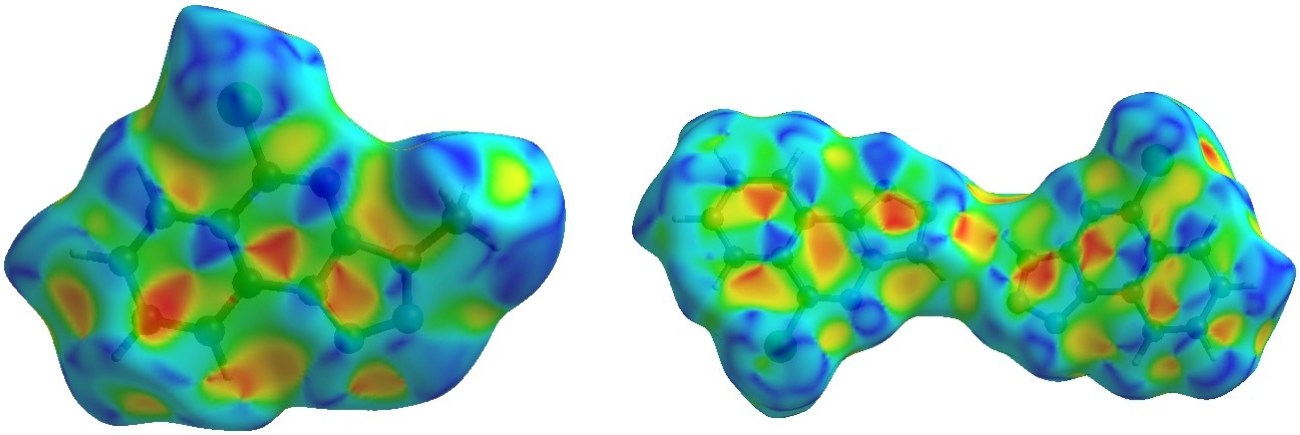

(a) **(b)**

Fig. S2. Hirshfeld surfaces of compounds **5** (Fig. S2a) and **6** (Fig. S2b) plotted over shape-index.

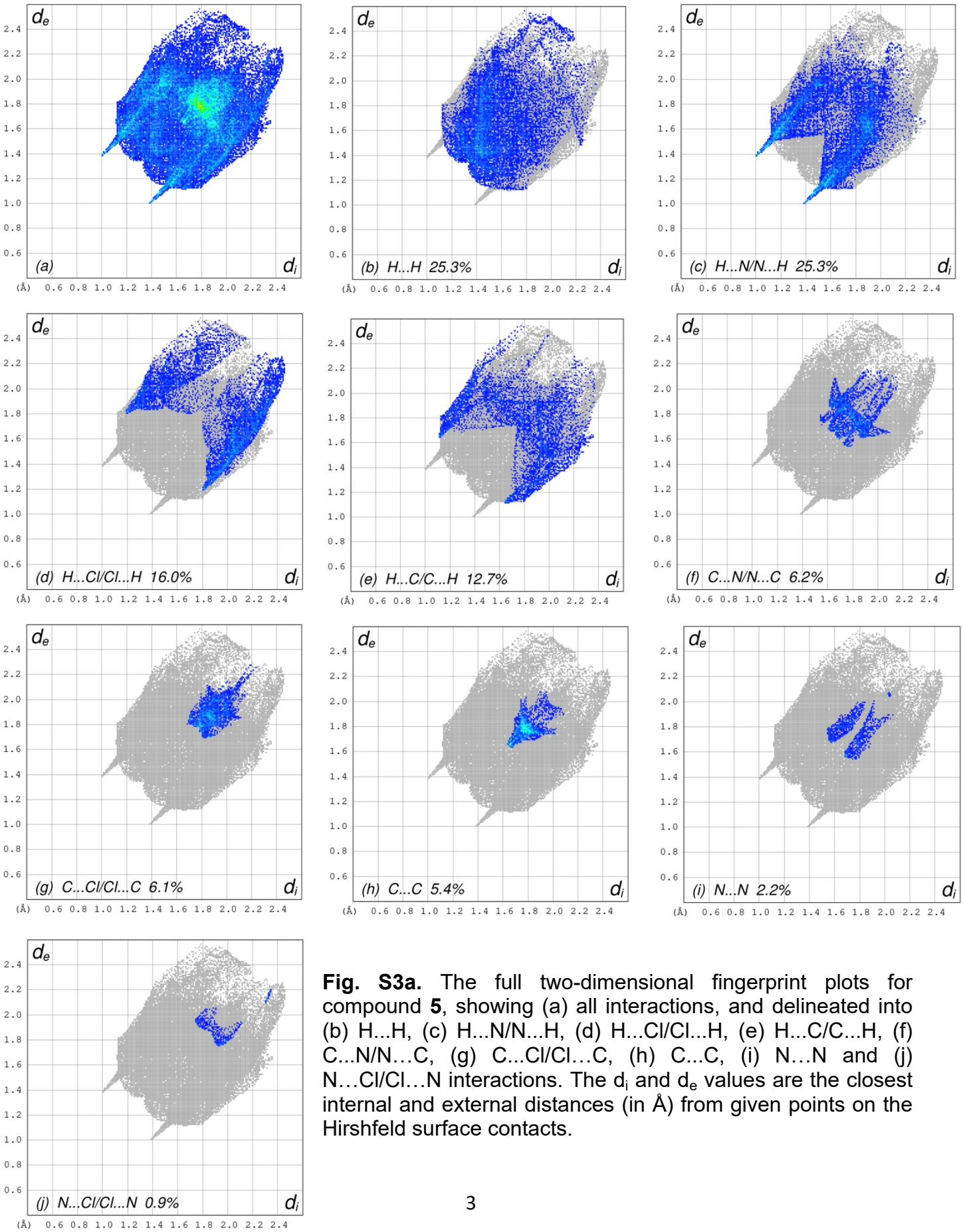

Fig. S3a. The full two-dimensional fingerprint plots for compound **5**, showing (a) all interactions, and delineated into (b) H...H, (c) H...N/N...H, (d) H...Cl/Cl...H, (e) H...C/C...H, (f) C...N/N…C, (g) C...Cl/Cl…C, (h) C...C, (i) N…N and (j) N…Cl/Cl…N interactions. The d_i and d_e values are the closest internal and external distances (in Å) from given points on the Hirshfeld surface contacts.

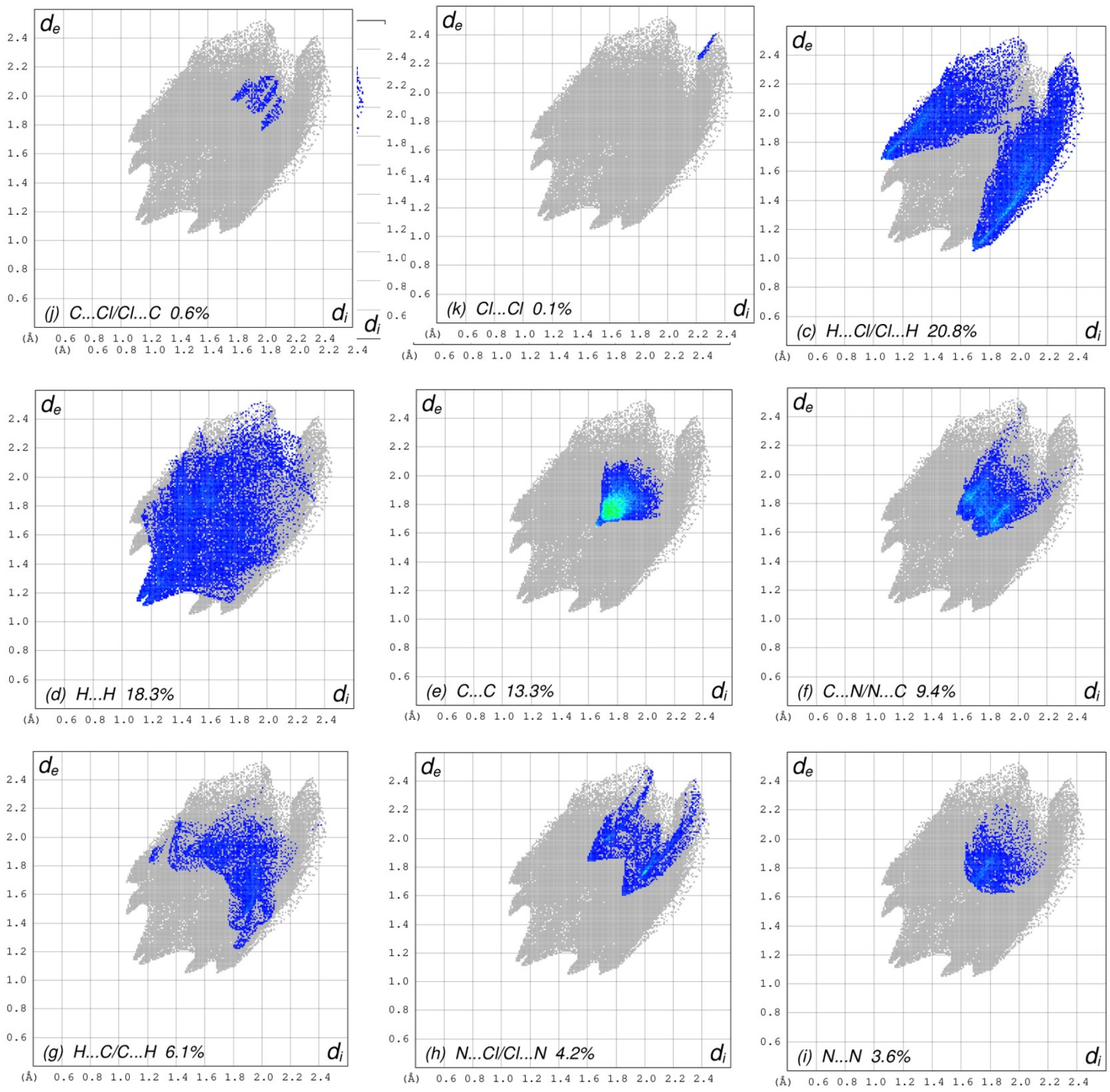
(j) C...Cl/Cl...C 0.6%
(k) Cl...Cl 0.1%
(c) H...Cl/Cl...H 20.8%
(d) H...H 18.3%
(e) C...C 13.3%
(f) C...N/N...C 9.4%
(g) H...C/C...H 6.1%
(h) N...Cl/Cl...N 4.2%
(i) N...N 3.6%
d_e
d_i
(Å) 0.6 0.8 1.0 1.2 1.4 1.6 1.8 2.0 2.2 2.4

Fig. S3b. The full two-dimensional fingerprint plots for compound **6**, showing (a) all interactions, and delineated into (b) H...N/N…H, (c) H...Cl/Cl...H, (d) H...H, (e) C…C, (f) C...N/N...C, (g) H...C/C…H, (h) N…Cl/Cl…N, (i) N…N, (j) C…Cl/Cl…C and (k) Cl…Cl interactions. The d_i and d_e values are the closest internal and external distances (in Å) from given points on the Hirshfeld surface contacts.

The overall two-dimensional fingerprint plots, Figs. S3 (a and b) a, and those delineated into H...H, H...N/N...H, H...Cl/Cl...H, H...C/C...H, C...N/N…C, C...Cl/Cl…C, C...C, N…N and N…Cl/Cl…N (for compound **5**) and H...N/N…H, H...Cl/Cl...H, H...H, C…C, C...N/N...C, H...C/C…H, N…Cl/Cl…N, C…Cl/Cl…C and Cl…Cl (for compound **6**) contacts [1] are illustrated in Figs. S3 (a) b-j (for compound **5**) and Figs. S3 (b) b-k (for compound **6**), together with their relative contributions to the Hirshfeld surfaces. The important interactions H...H contribute 25.3% (for **5**) and 18.3% (for **6**) to the overall crystal packing, which are reflected in Figs. S3 (a and b) b (for **5**) and d (for **6**) as the widely scattered points of high density due to the large hydrogen contents of the molecules with the tips at $d_e = d_i = 1.33$ Å (for **5**) and $d_e = d_i = 1.13$ Å (for **6**). The pairs of characteristic wings resulting in the fingerprint plots delineated into H...N/N...H, Figs. S3 (a and b) c (for **5**) and b (for **6**) contacts with 25.3% (for **5**) and 23.7% (for 6) contributions to the HSs are viewed as pairs of spikes with the tips at $d_e + d_i = 2.38$ Å (for **5**) and $d_e + d_i = 2.52$ Å (for 6). The H...Cl/Cl...H contacts contributing 16.0% (for **5**) and 20.8% (for **6**) to the overall crystal packing, are reflected in Figs. S3 (a and b) d (for **5**) and c (for **6**) with the tips at at $d_e + d_i = 2.98$ Å (for **5**) and $d_e + d_i = 2.73$ Å (for 6). In the absence of C-H...π interactions (for **5** and **6**), the H...C/C...H contacts contributing 12.7% (for **5**) and 6.1% (for **6**) to the overall crystal packing, are reflected in Figs. S3 (a and b) e (for **5**) and g (for **6**) with the tips of the wings at $d_e + d_i = 2.76$ Å (for **5**) and $d_e + d_i = 3.17$ Å (for **6**). The C...N/N...C contacts contributing 6.2% (for **5**) and 9.4% (for **6**) to the overall crystal packing, are reflected in Figs. S3 (a and b) f (for **5**) and f (for **6**) with the tips of the tiny wings at $d_e + d_i = 3.30$ Å (for **5**) and $d_e + d_i = 3.30$ Å (for **6**). The C...Cl/Cl...C (in **5**) and N...Cl/Cl...N (in **6**) contacts contribute 6.1% (for **5**) and 4.2% (for **6**) to the overall crystal packing, and they are reflected in Figs. S3 (a and b) g (for **5**) and h (for **6**) with the tips of the wings at $d_e + d_i = 3.48$ Å (for **5**) and $d_e + d_i = 3.45$ Å (for **6**). The C...C contacts with 5.4% (for **5**) and 13.3% (for

6) contributions to the HSs are viewed as arrow-shaped distributions of points with the tips at $d_e = d_i = 1.64$ Å (for **5**) and $d_e = d_i = 1.63$ Å (for **6**), and they are reflected in Fig. S3 (a) h (for **5)** and Fig. S3 (b) e (for **6**). The N...N contacts with 2.2% (for **5**) and 3.6% (for **6**) contributions to the HSs are viewed with the tips at $d_e + d_i = 3.23$ Å (for **5**) and $d_e = d_i = 1.68$ Å (for **6**), and they are reflected in Fig. S3 (a) i (for **5)** and Fig. S3 (b) i (for **6**). The contributions of the remaining N...Cl/Cl...N (for **5**) and C...Cl/Cl...C and Cl…Cl (for **6**) contacts Figs. S3 (a and b) are smaller than 1.0% to the HSs with the low densities of points.

The Hirshfeld surface representations with the function d_{norm} plotted onto the surfaces are shown for the H...H, H...N/N...H, H...Cl/Cl...H and H...C/C...H (for **5**) and H...N/N…H, H...Cl/Cl...H, H…H, C…C and C…N/N…C (for **6**) interactions in Fig. S4 and Fig. S5, respectively.

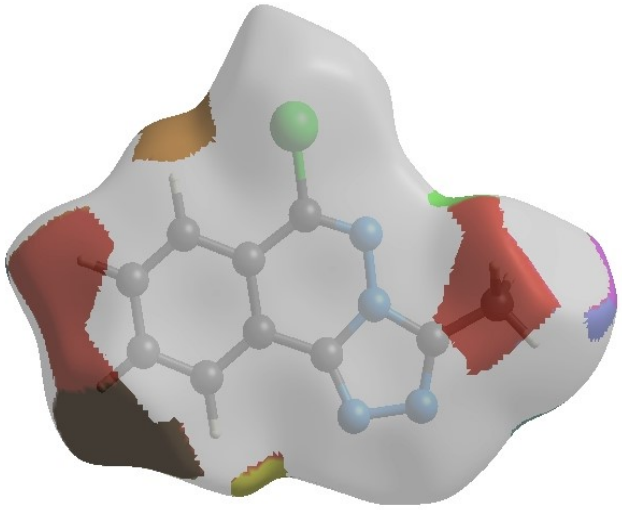

(a)

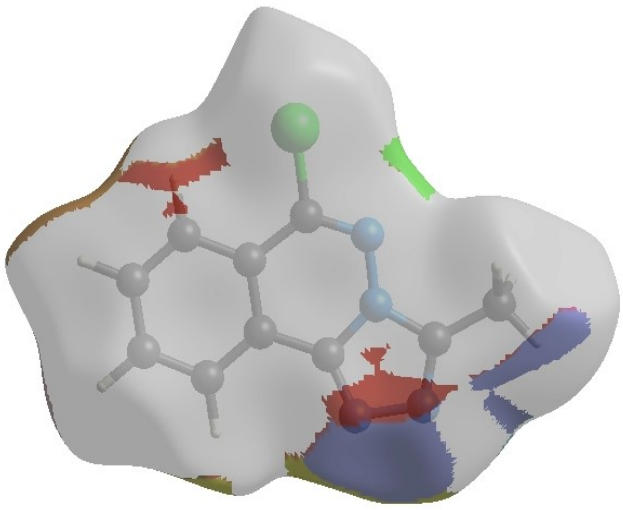

(b)

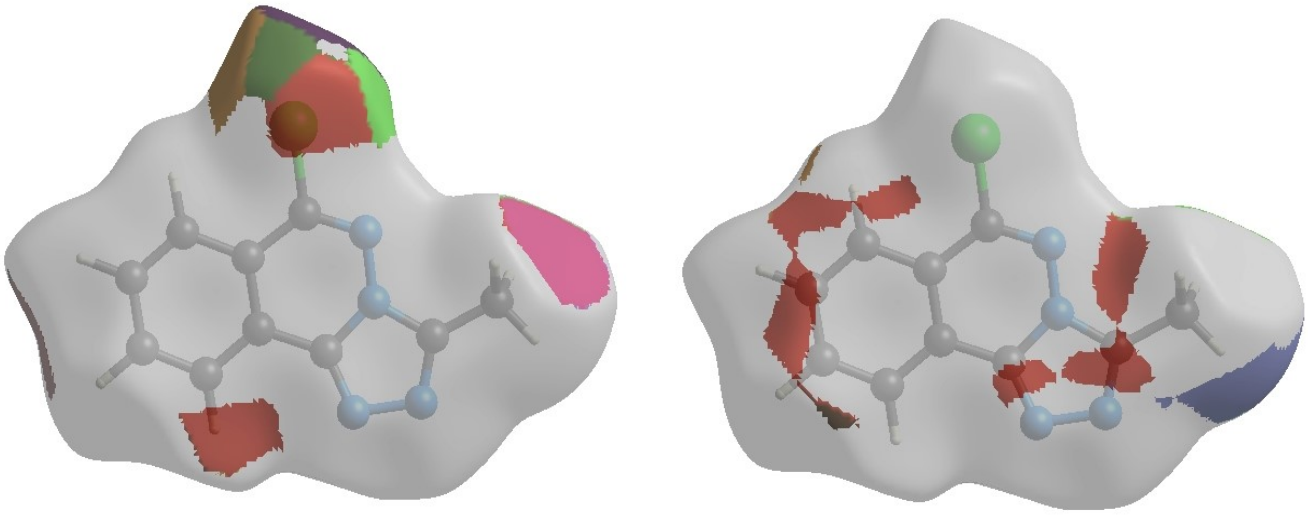

(c) **(d)**

Fig. S4. The Hirshfeld surface representations of compound **5** with the function d_{norm} plotted onto the surface for (a) H...H, (b) H...N/N...H, (c) H...Cl/Cl...H and (d) H...C/C...H interactions.

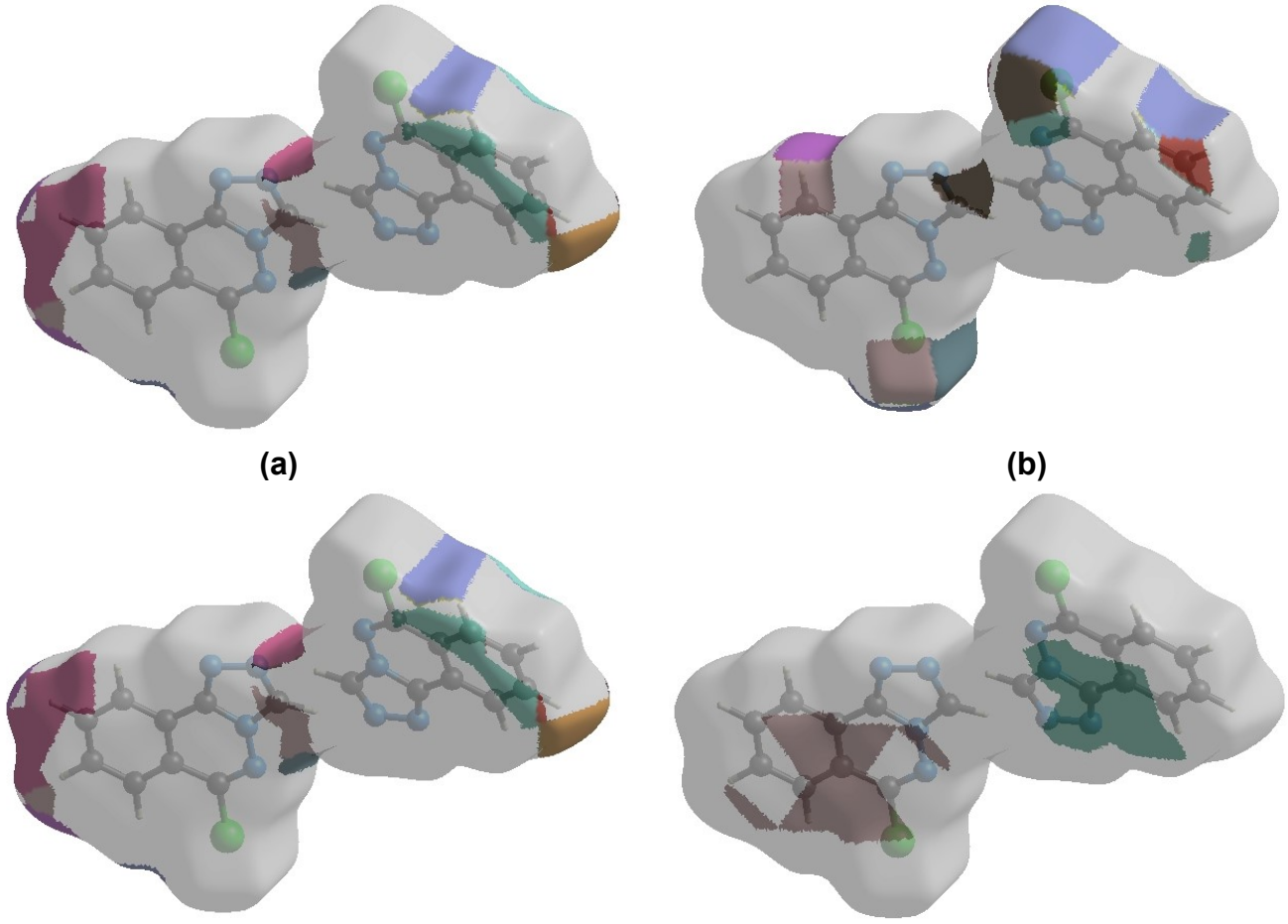

(a) **(b)**

(c) **(d)**

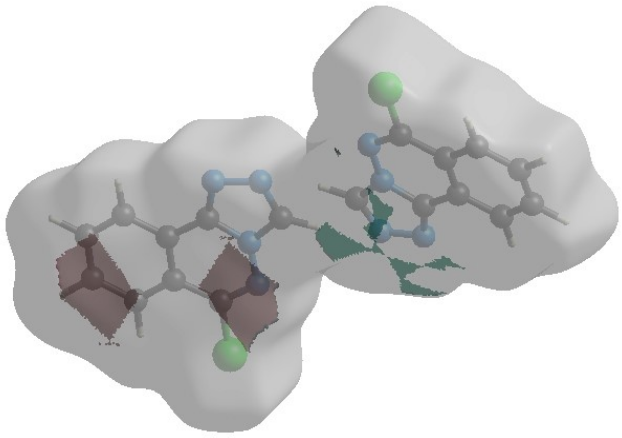

(e)

Fig. S5. The Hirshfeld surface representations of compound **6** with the function d_{norm} plotted onto the surface for (a) H...N/N…H, (b) H...Cl/Cl...H, (c) H…H, (d) C…C and (e) C…N/N…C interactions.

The Hirshfeld surface analyses confirm the importance of H-atom contacts in establishing the packing. The large number of H...H, H...C/C...H, H...Cl/Cl...H and H...N/N...H interactions suggest that van der Waals interactions and hydrogen bonding play the major roles in the crystal packing [2].

Crystal voids

The strength of the crystal packing is highly important to response to the applied mechanical force depending on the “how crystal packing is strong”. Of course that, if the crystal packing have large empty spaces, then the molecules are not tightly packed and a small amount of the applied external mechanical force may break the crystal easily. For checking the mechanical stability of the crystal packing, void analysis was performed by adding up the electron densities of the spherically symmetric atoms contained in the asymmetric unit [3]. The void surface is defined as an isosurface of the procrystal electron density, and calculated for the whole unit cell. Where the void surface meets the boundary of the unit cell, and the capping faces are generated to create an enclosed volume. The volumes of the crystal voids (Fig. S6) and the percentages of free spaces in the unit cells are calculated as 68.28 $Å^3$ and 7.37% (for **5**) and 91.46 $Å^3$ and 5.61% (for **6**). Thus, there is not any large cavity in the crystal packing.

Interaction energy calculations

The intermolecular interaction energies are calculated using CE–B3LYP/6–31G(d,p) energy model available in Crystal Explorer 17.5 [4], where a cluster of molecules is generated by applying crystallographic symmetry operations with respect to a selected central molecule

within the radius of 3.8 Å by default [5]. The total intermolecular energy (E_{tot}) is the sum of electrostatic (E_{ele}), polarization (E_{pol}), dispersion (E_{dis}) and exchange-repulsion (E_{rep}) energies [6] with scale factors of 1.057, 0.740, 0.871 and 0.618, respectively [7]. Hydrogen-bonding interaction energies (in kJ mol^{-1}) are -13.3 (E_{ele}), -1.9 (E_{pol}), -82.1 (E_{dis}), 60.0 (E_{rep}) and -49.9 (E_{tot}) (for C6-H6…N1) in compound **5**.

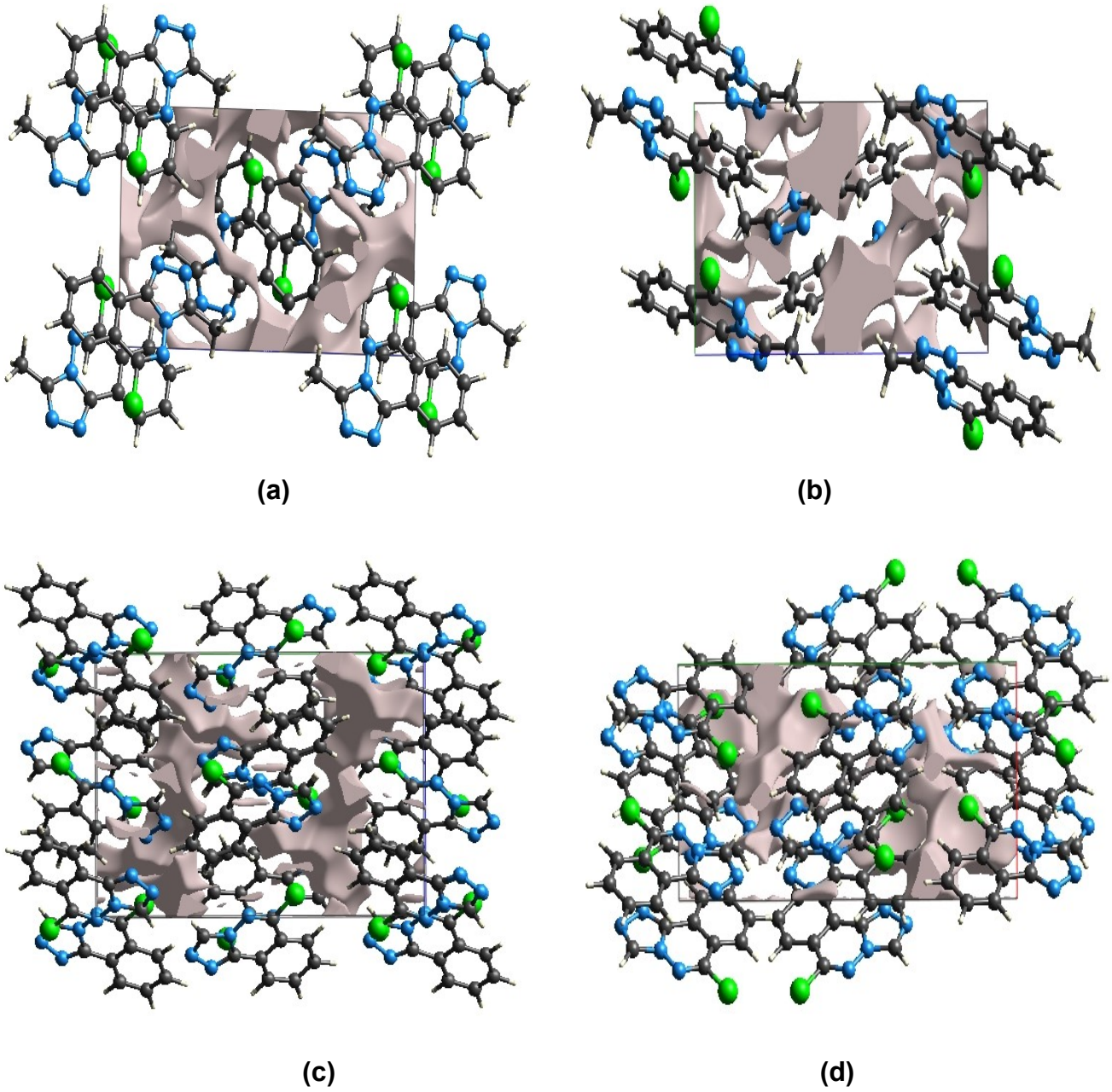

Fig. S6. Graphical views of voids in the crystal packings of compounds **5** and **6** [(a) along a-axis and (b) along b-axis (for **5**)] and [(c) along a-axis and (d) along c-axis (for **6**)].

Energy frameworks

Energy frameworks combine the calculation of intermolecular interaction energies with a graphical representation of their magnitude [6]. Energies between molecular pairs are represented as cylinders joining the centroids of pairs of molecules with the cylinder radius proportional to the relative strength of the corresponding interaction energy. Energy frameworks are constructed for E_{ele} (red cylinders), E_{dis} (green cylinders) and E_{tot} (blue cylinders) (Fig. S7). The evaluations of the electrostatic, dispersion and total energy frameworks indicate that the stabilizations are dominated via the dispersion energy contribution in compound **5** and the electrostatic energy contribution in compound **6**.

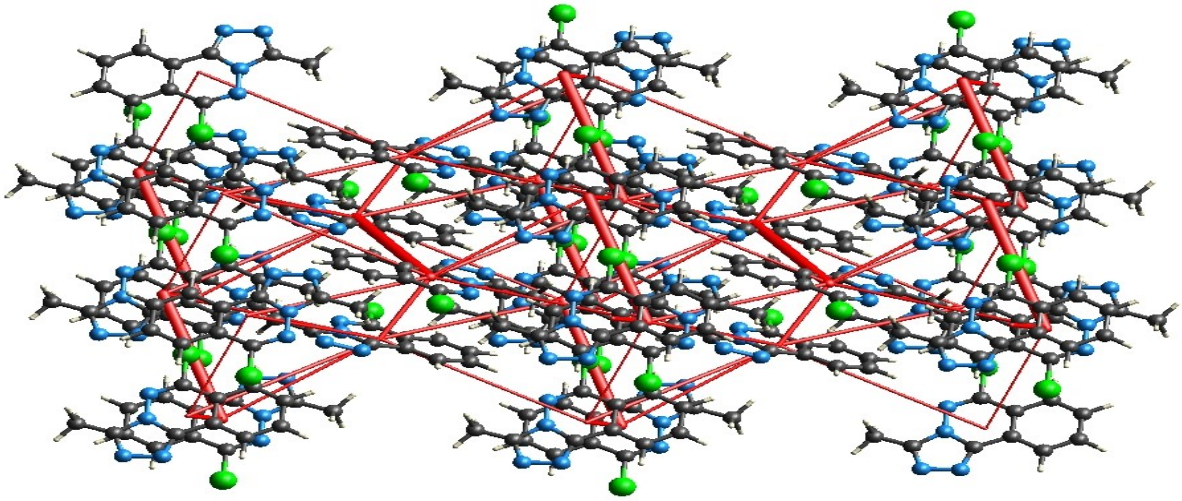

(a)

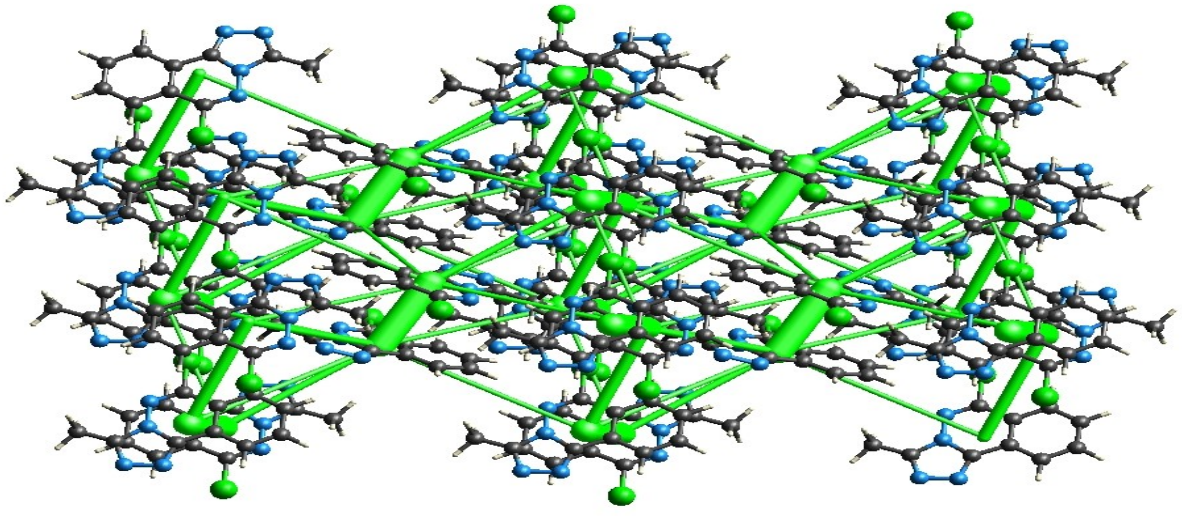

(b)

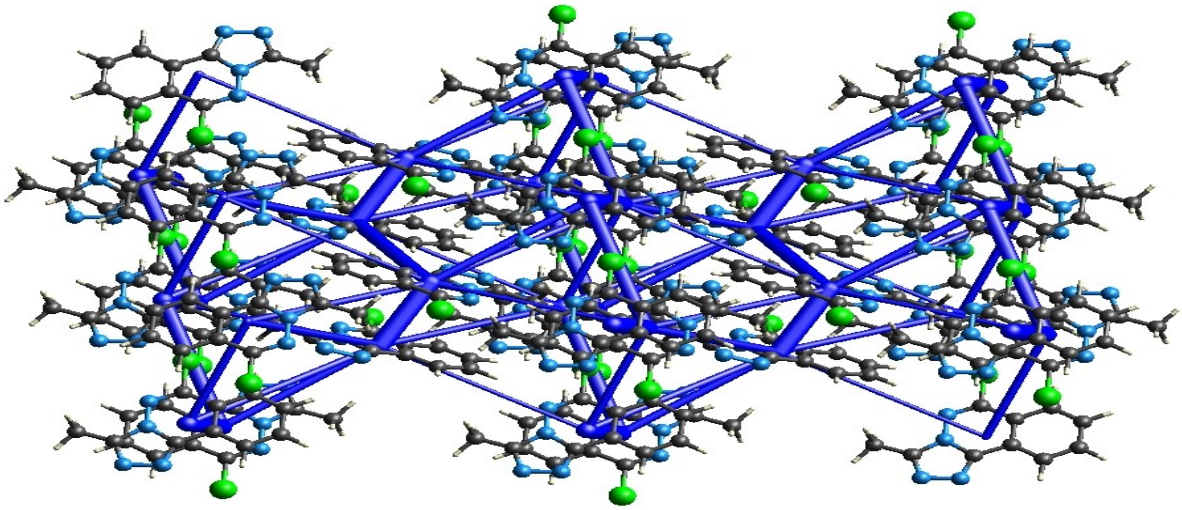

(c)

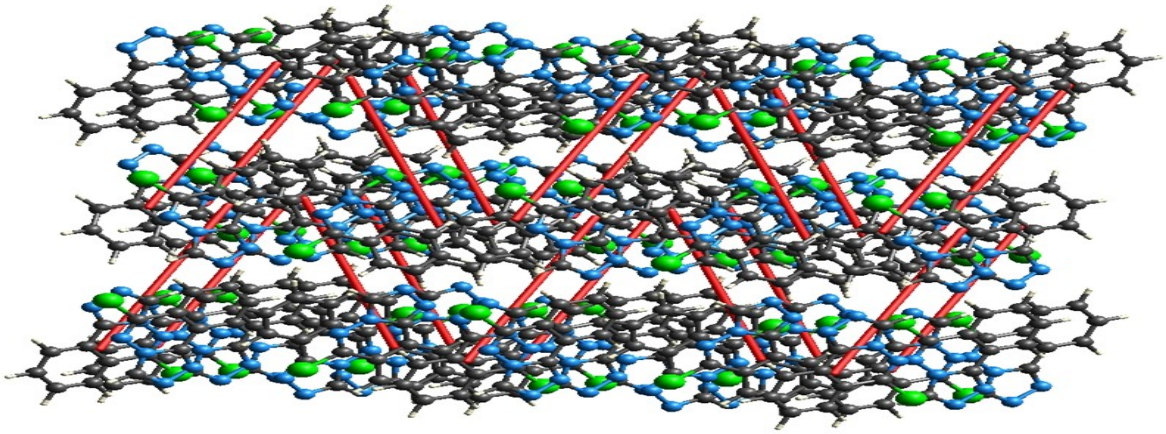

(d)

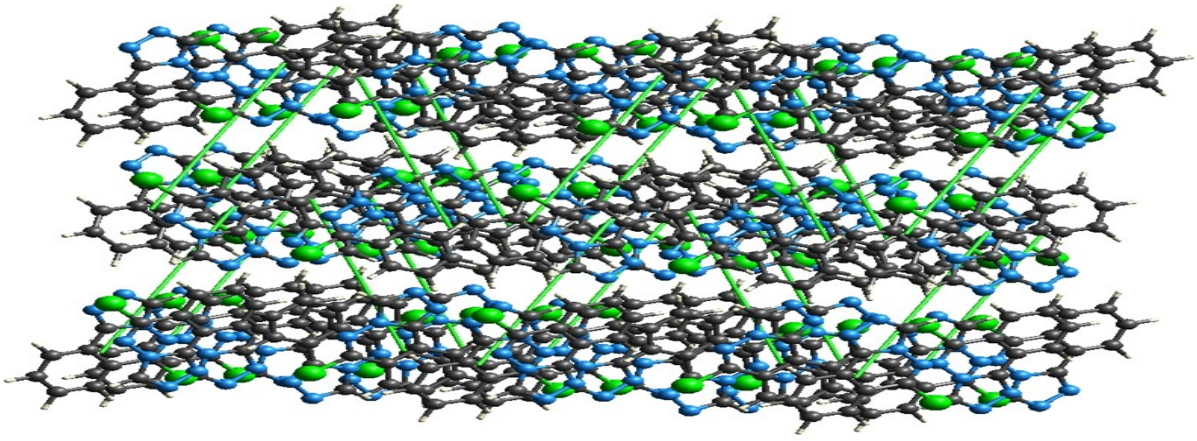

(e)

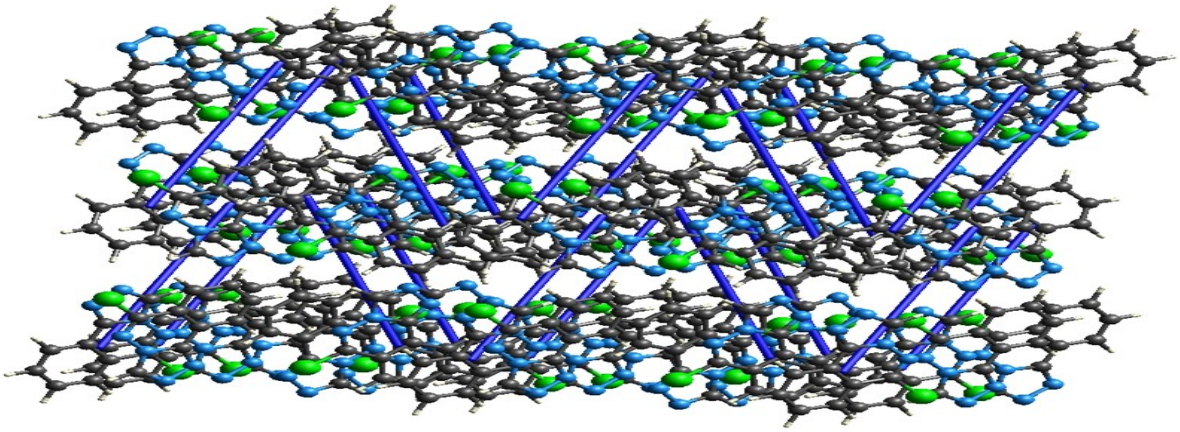

(f)

Fig. S7. Perspective views of the energy frameworks for a cluster of molecules of compounds (**5** and **6)** showing the [(a) (for **5**) and (d) (for **6**)] electrostatic energy, [(b) (for **5**), and (e) (for **6**)] dispersion energy and [(c) (for **5**) and (f) (for **6**)] total energy diagrams. The cylindrical radius is proportional to the relative strength of the corresponding energies and they were adjusted to the same scale factor of 80 with cut-off value of 5 kJ mol^{-1} within 2 X 1 X 2 unit cells.

Molecular docking

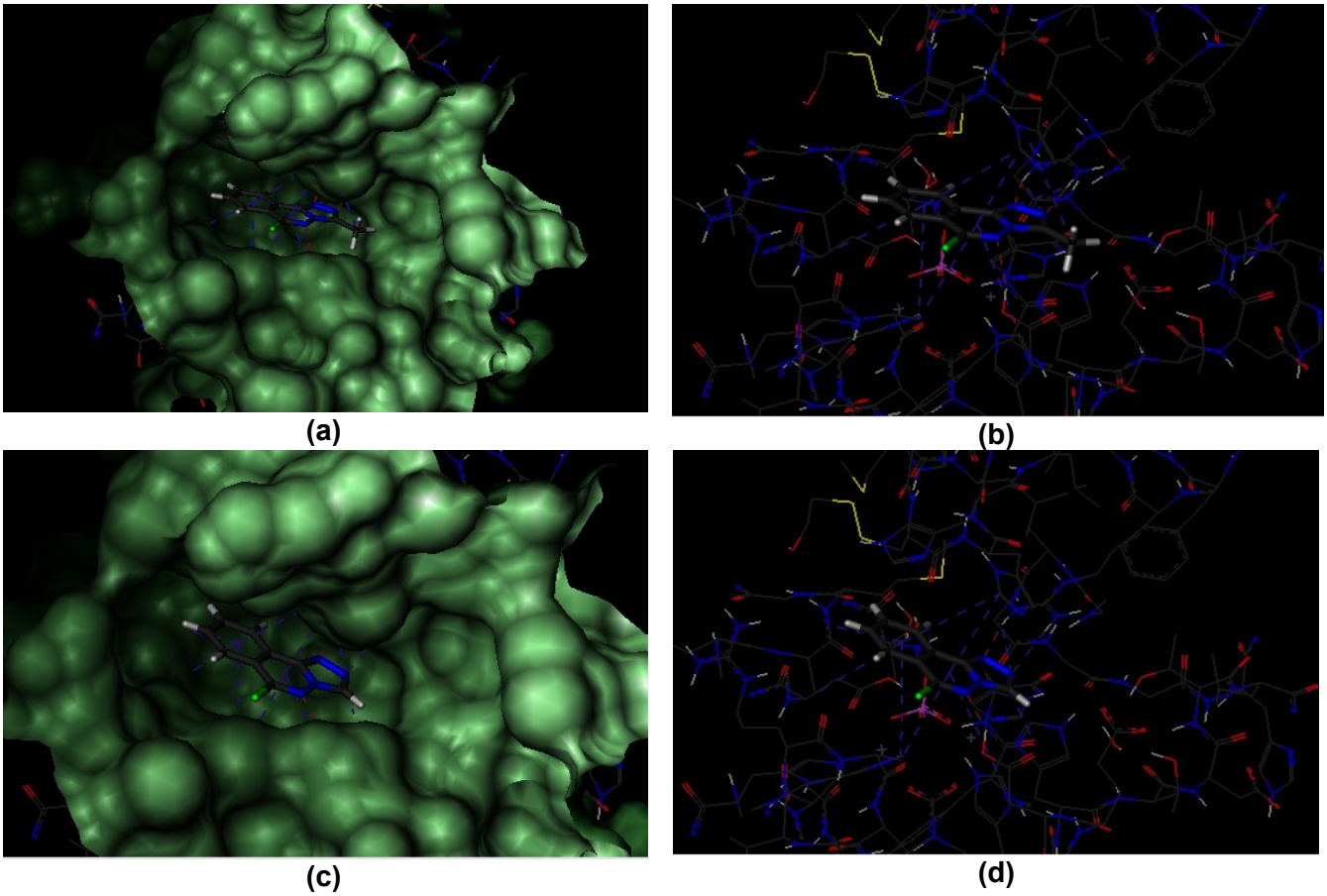

Figure S8. Docked poses of compound **5** (a-b) and **6** (c-d) within the active pocket of urease with and without surface depicted by Biosolve LeadIT.

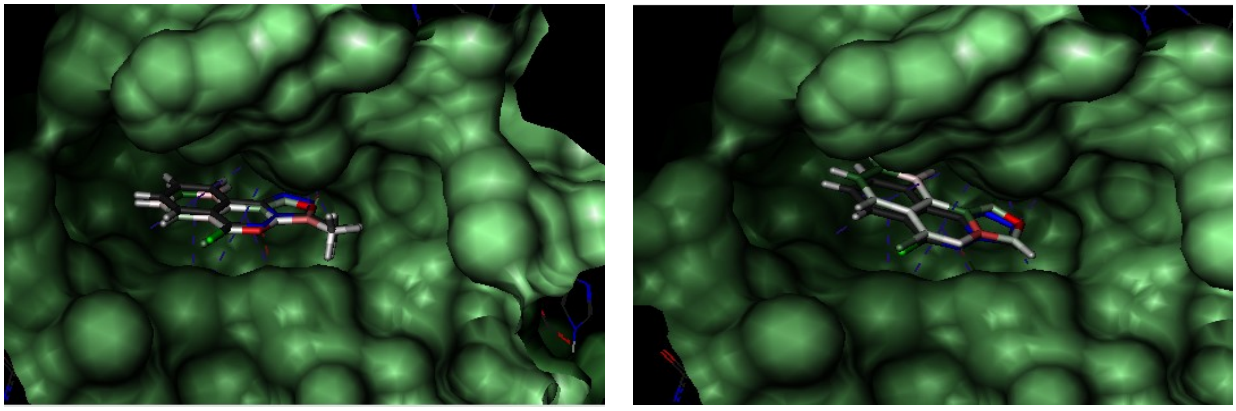

(a) **(b)**

Fig. S9. Docked pocket of urease showing the poses selected for HYDE calculations. Pose # 3 of compound **5** (a), and pose # 1 of compound **6** (b) predicting the complete superimposition of docked poses having "scoring", i.e., the affinity assessment of a ligand in a binding pocket.

Table S1 ADME properties of compounds **5** and **6**.

Properties	Compounds	
	5	**6**
Physicochemical properties		
Molecular weight (g/mol)	218.64	204.62
No. of heavy atoms	15	14
No. of aromatic heavy atoms	13	13
Fraction C_{sp3}	0.10	0
No. of rotatable bonds	0	0
No. of H-bond acceptors	3	3
No. of H-bond donors	0	0
Molar refractivity	58.26	53.30
TPSA (Å^2)	43.08	43.08
Lipophilicity		
Log $P_{o/w}$ (iLOGP)	2.10	1.77
Log $P_{o/w}$ (XLOGP3)	2.35	1.95
Log $P_{o/w}$ (WLOGP)	2.24	1.93
Log $P_{o/w}$ (MLOGP)	2.86	2.17
Log $P_{o/w}$ (SILICOS-IT)	1.98	1.54
Consensus Log $P_{o/w}$	2.31	1.87
Water solubility		
Log S (ESOL)	–3.32	–3.02
Solubility (mg/mL; mol/L)	1.05e-01; 4.81e-04	1.93e-01; 9.46e-04
Class	Soluble	Soluble
Log S (ALi)	–2.89	–2.48
Solubility(mg/ml; mol/l)	2.79e-01; 1.28e-03	6.78e-01; 3.32e-03
Class	Soluble	Soluble
Log S (SILICOS-IT)	–4.03	–3.64
Solubility (mg/ml; mol/l)	2.05e-02; 9.40e-05	4.71e-02; 2.30e-04

Class	Moderately soluble	Soluble
Pharmacokinetics		
GI absorption	High	High
BBB permeant	Yes	Yes
P-gp substrate	No	No
CYP1A2 inhibitor	Yes	Yes
CYP2C19 inhibitor	No	No
CYP2C9 inhibitor	No	No
CYP2D6 inhibitor	No	No
CYP3A4 inhibitor	No	No
Log K_p (skin permeation) (cm/s)	–5.97	–6.16
Druglikeness		
Lipinski	Yes; 0 violation	Yes; 0 violation
Ghose	Yes; 0 violation	No; 1 violation:#atoms<20
Veber	Yes; 0 violation	Yes; 0 violation
Egan	Yes; 0 violation	Yes; 0 violation
Muegge	Yes; 0 violation	Yes; 0 violation
Bioavailability score	0.55	0.55
Medicinal chemistry		
PAINS	0 alert	0 alert
Brenk	0 alert	0 alert
Leadlikeness	No; 1 Violation MW<250	No; 1 Violation MW<250
Synthetic accessibility	2.14	1.90

References

[1] J. J. McKinnon, D. Jayatilaka and M. A. Spackman, *Chem. Commun.,* 2007, **37**, 3814-3816.

[2] V. R. Hartwar, M. Sist, M. R. V. Jorgensen, A. H. Mamakhel, X. Wang, C. M. Hoffmann, K. Sugimoto, J. Overgaard, B. B. Iversen, *IUCrJ,* 2015, **2**, 563-574.

[3] M. J. Turner, J. J. McKinnon, D. Jayatilaka and M. A. Spackman, *CrystEngComm,* 2011, **13**, 1804-1813.

[4] M. J. Turner, J. J. McKinnon, S. K. Wolff, D. J. Grimwood, P. R. Spackman, D. Jayatilaka and M. A. Spackman, M. A. Crystal Explorer17, 2017. The University of Western Australia, Nedlands, Western Australia; http://hirshfeldsurface.net.

[5] M. J. Turner, S. Grabowsky, D. Jayatilaka and M. A. Spackman, *J. Phys. Chem. Lett.*, 2014, **5**, 4249-4255.

[6] M. J. Turner, S. P. Thomas, M. W. Shi, D. Jayatilaka and M. A. Spackman, *Chem. Commun.,* 2015, **51**, 3735-3738.

[7] C. F. Mackenzie, P. R. Spackman, D. Jayatilaka and M. A. Spackman, *IUCrJ,* 2017, **4**, 575-587.

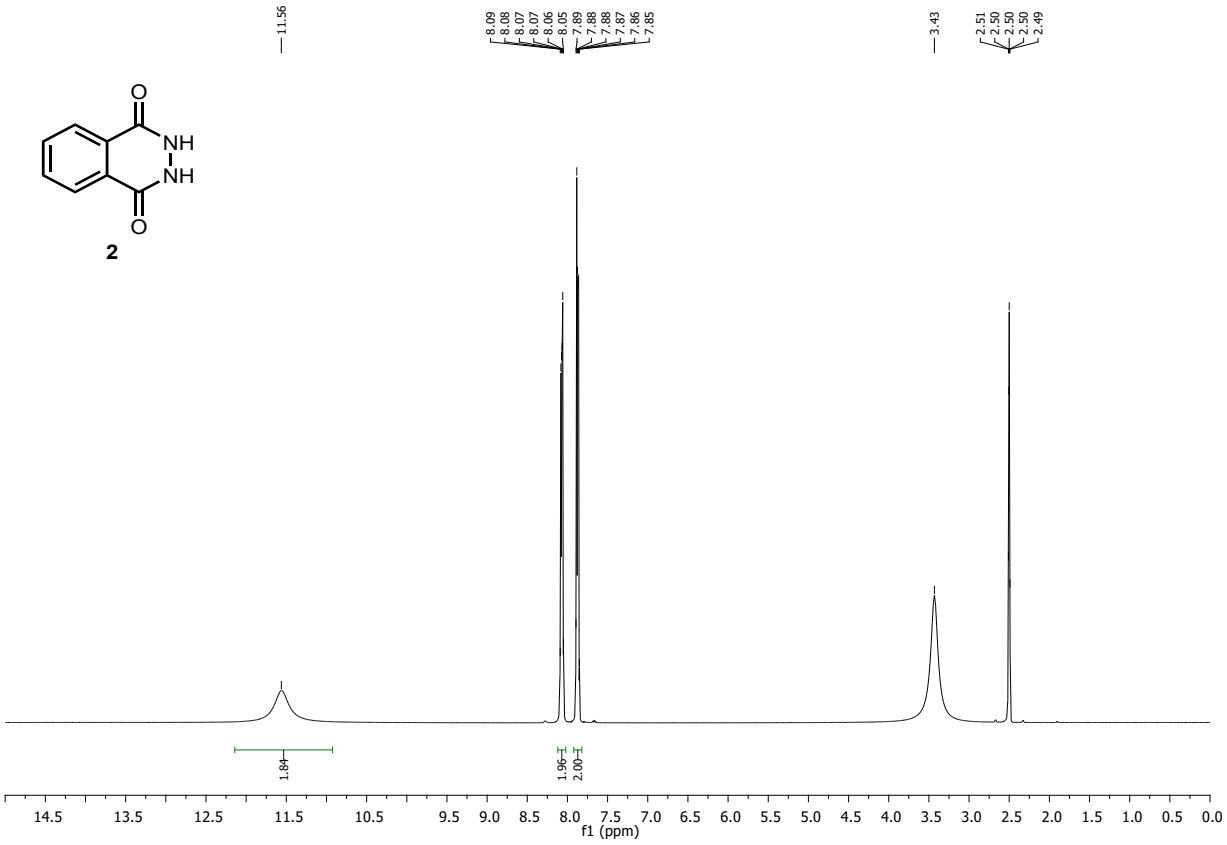
11.56
8.09
8.08
8.07
8.07
8.06
8.05
7.89
7.88
7.88
7.87
7.86
7.85
3.43
2.51
2.50
2.50
2.50
2.49
1.84
1.96
2.00
14.5
13.5
12.5
11.5
10.5
9.5
9.0
8.5
8.0
7.5
7.0
6.5
6.0
5.5
5.0
4.5
4.0
3.5
3.0
2.5
2.0
1.5
1.0
0.5
0.0
f1 (ppm)

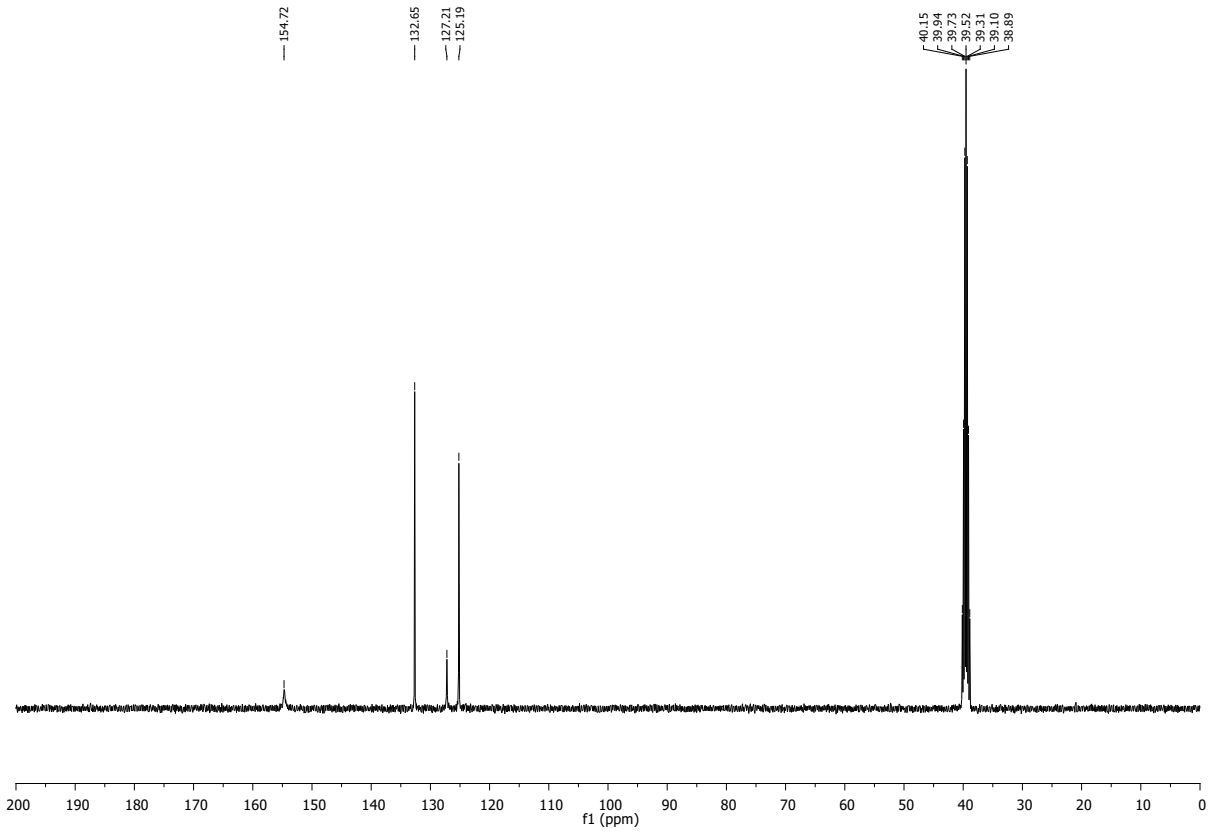
154.72
132.65
127.21
125.19
40.15
39.94
39.73
39.52
39.31
39.10
38.89
200
190
180
170
160
150
140
130
120
110
100
90
80
70
60
50
40
30
20
10
0
f1 (ppm)

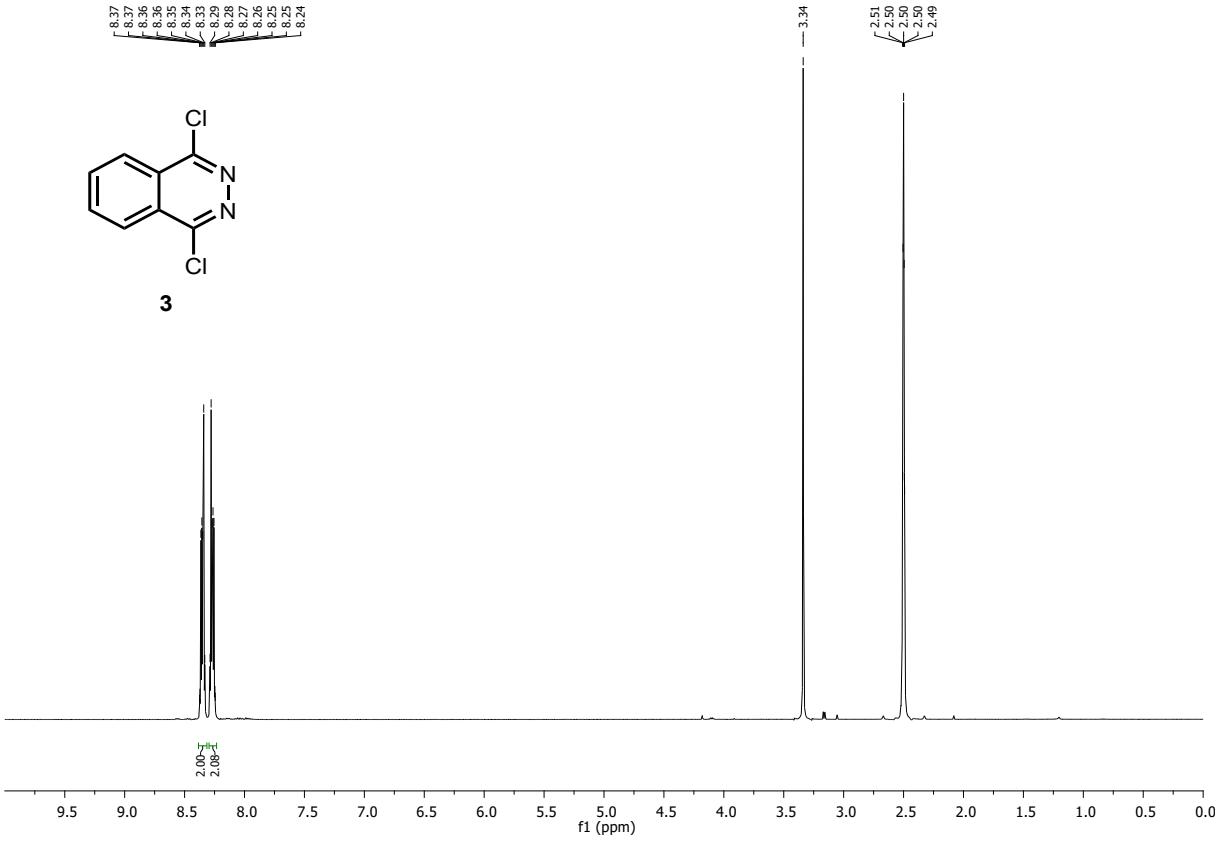
8.37
8.37
8.36
8.36
8.35
8.34
8.33
8.29
8.28
8.27
8.26
8.25
8.25
8.24
3.34
2.51
2.50
2.50
2.50
2.49
Cl
N
N
Cl
2.00
2.08
9.5 9.0 8.5 8.0 7.5 7.0 6.5 6.0 5.5 5.0 4.5 4.0 3.5 3.0 2.5 2.0 1.5 1.0 0.5 0.0
f1 (ppm)

3

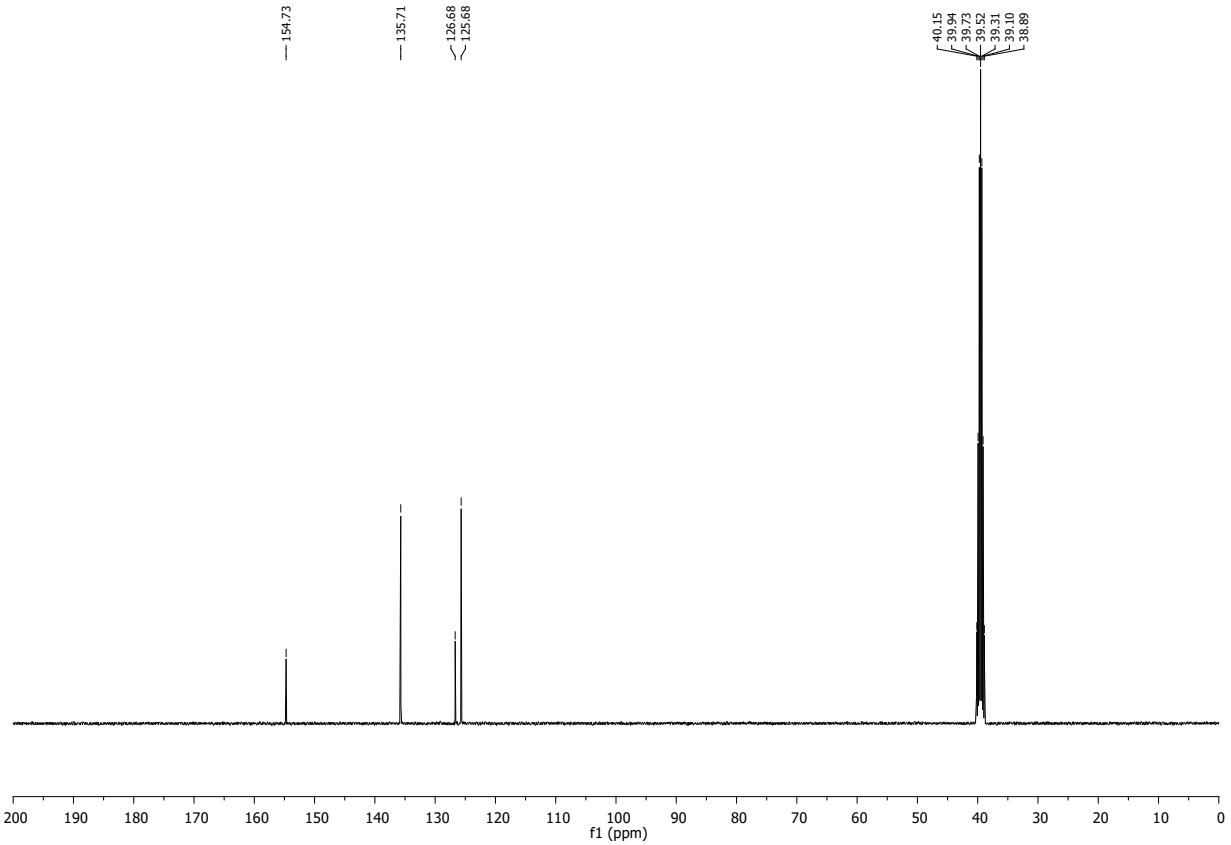
154.73
135.71
126.68
125.68
40.15
39.94
39.73
39.52
39.31
39.10
38.89
200 190 180 170 160 150 140 130 120 110 100 90 80 70 60 50 40 30 20 10 0
f1 (ppm)

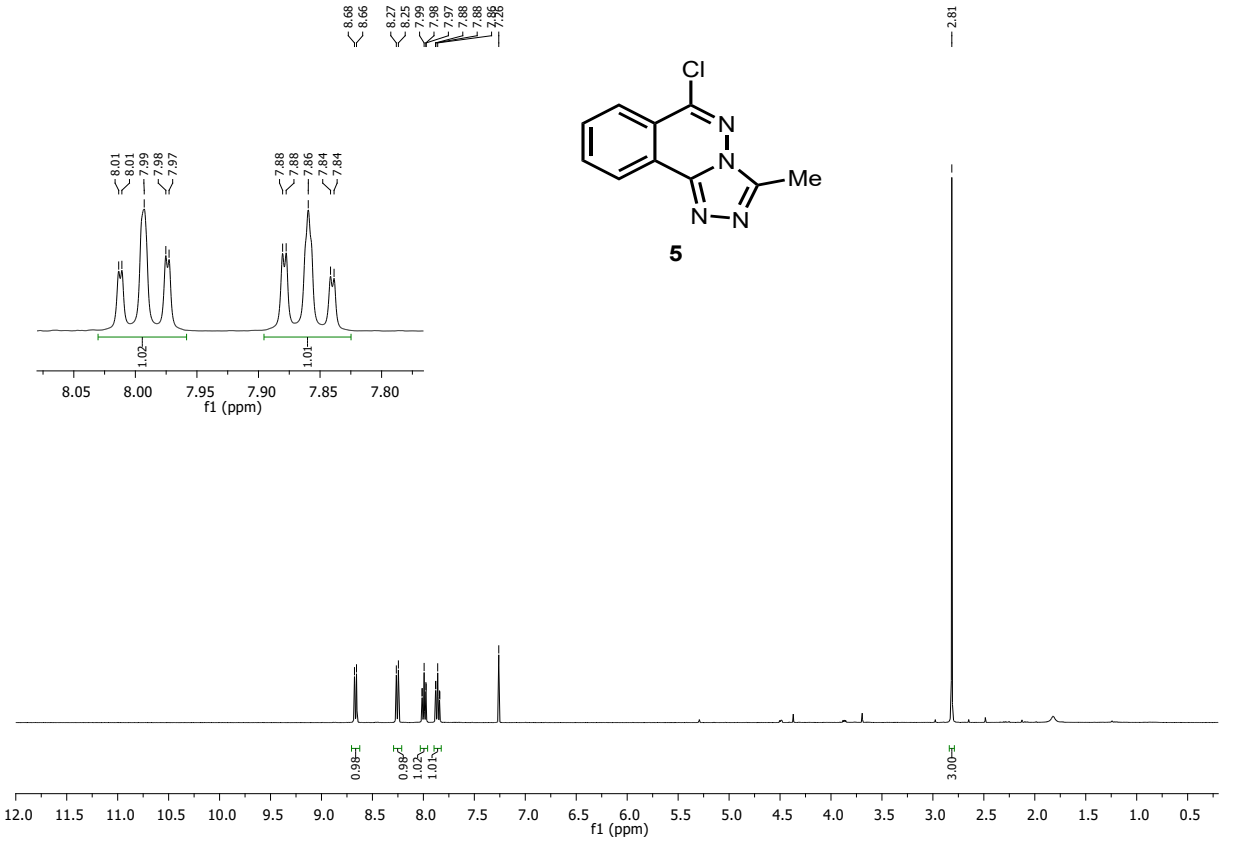
8.68
8.66
8.27
8.25
7.99
7.98
7.97
7.88
7.88
7.86
7.84
7.84
2.81
8.01
8.01
7.99
7.98
7.97
7.88
7.88
7.86
7.84
7.84
1.02
1.01
8.05
8.00
7.95
7.90
7.85
7.80
f1 (ppm)
Cl
N
N
Me
N
N
0.98
0.98
1.02
1.01
3.00
12.0
11.5
11.0
10.5
10.0
9.5
9.0
8.5
8.0
7.5
7.0
6.5
6.0
5.5
5.0
4.5
4.0
3.5
3.0
2.5
2.0
1.5
1.0
0.5
f1 (ppm)

5

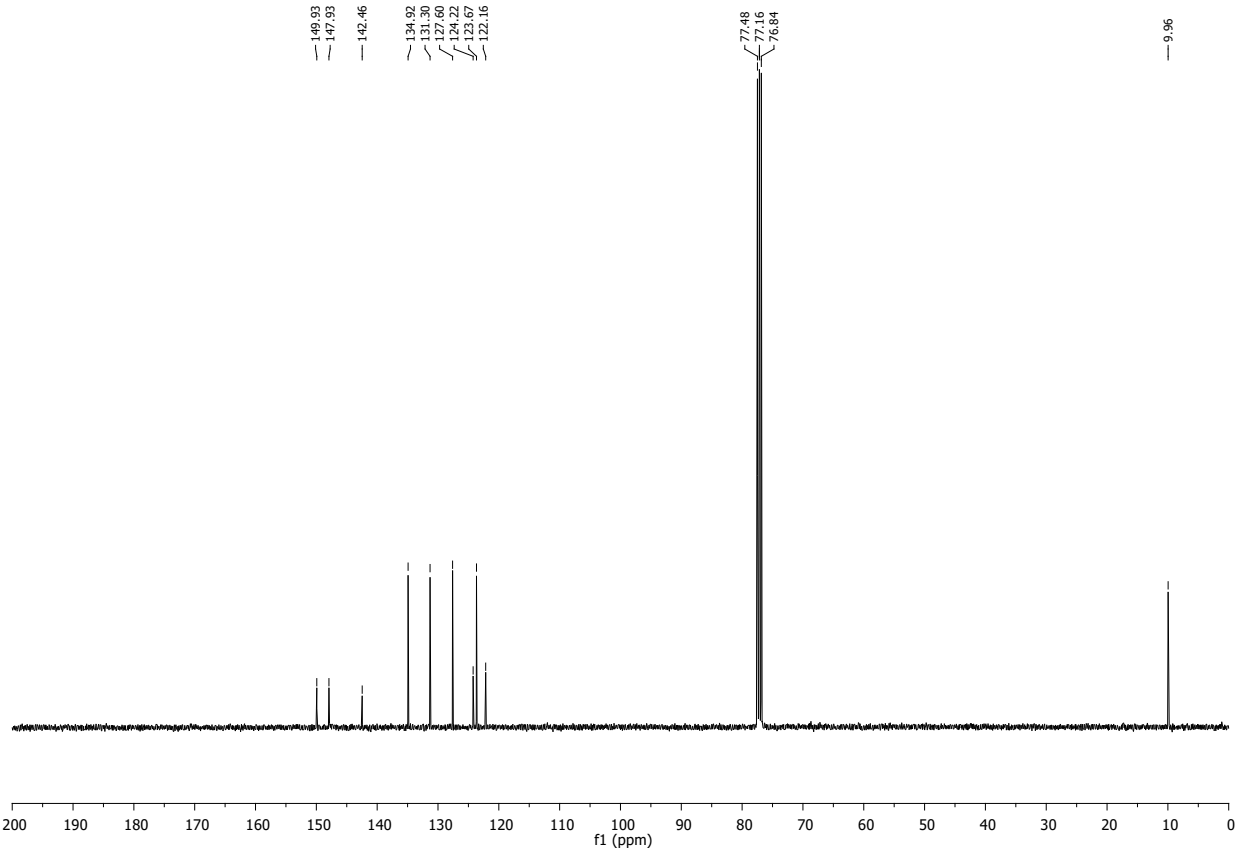
149.93
147.93
142.46
134.92
131.30
127.60
124.22
123.67
122.16
77.48
77.16
76.84
9.96
200
190
180
170
160
150
140
130
120
110
100
90
80
70
60
50
40
30
20
10
0
f1 (ppm)

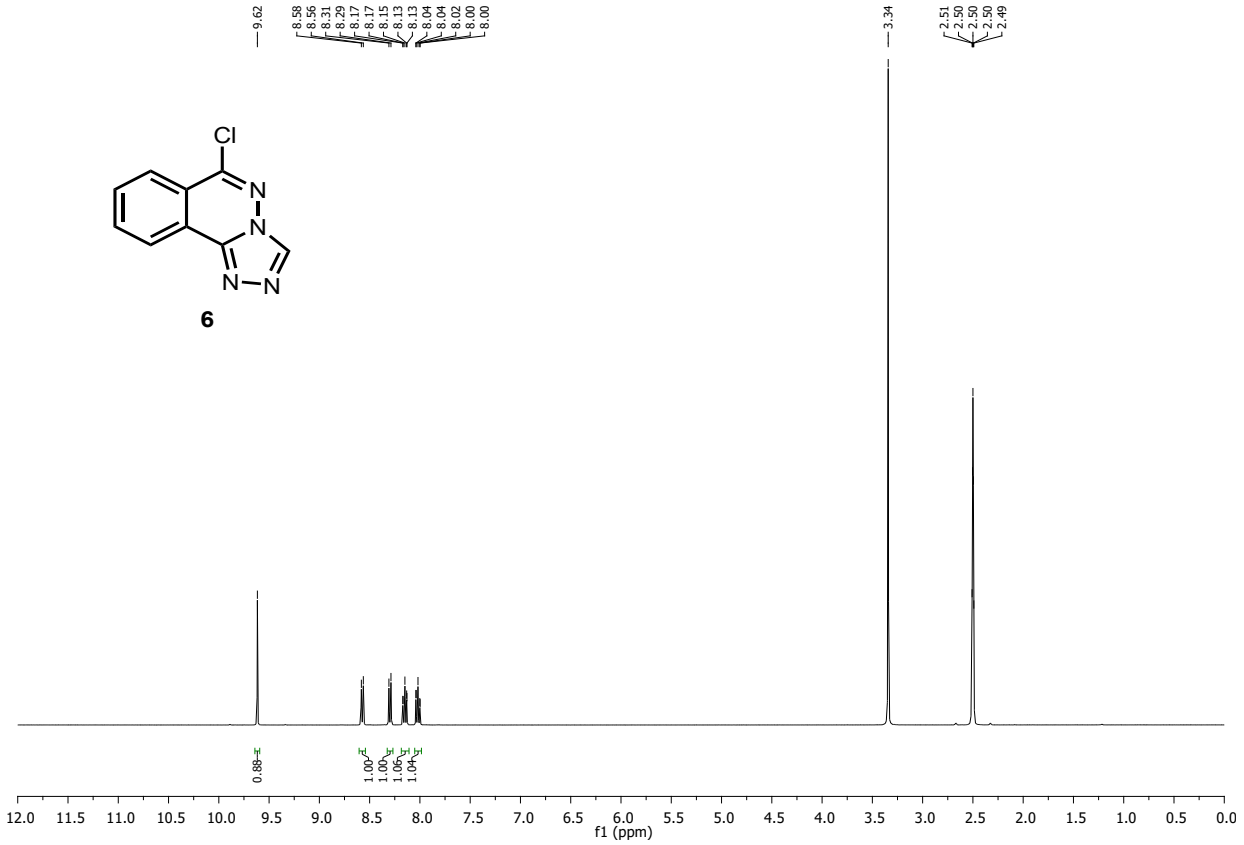
9.62
8.58
8.56
8.31
8.29
8.17
8.17
8.15
8.13
8.13
8.04
8.04
8.02
8.00
8.00
3.34
2.51
2.50
2.50
2.50
2.49
Cl
N
N
N
N
0.88
1.00
1.00
1.06
1.06
1.04
f1 (ppm)

6

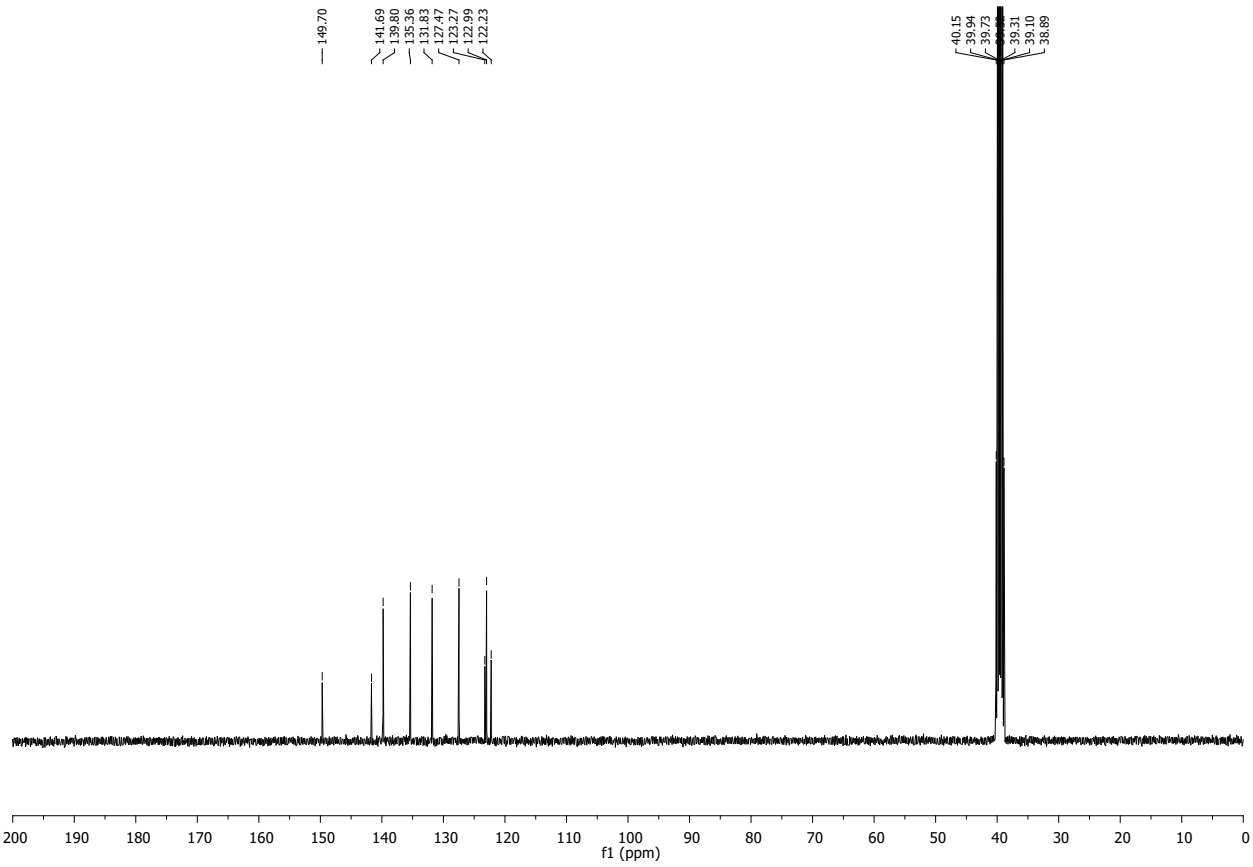
149.70
141.69
139.80
135.36
131.83
127.47
123.27
122.99
122.23
40.15
39.94
39.73
39.31
39.10
38.89
f1 (ppm)